Spectrochimica Acta Part A: Molecular and Biomolecular Spectroscopy 123 (2014) 46–53

Contents lists available at ScienceDirect

Spectrochimica Acta Part A: Molecular and Biomolecular Spectroscopy

journal homepage: www.elsevier.com/locate/saa

Synthesis and nonlinear optical properties in the near-IR range of stilbazolium dyes

Fuying Hao *, Dongpo Zhu, Jilong Ma, Lanlan Chai

Department of Chemistry, Fuyang Normal College, Fuyang 236036, China

HIGHLIGHTS

- The molecular geometry optimization for calculation results from the structure.
- The dyes exhibit two-photon absorption in near-infrared range.
- The dyes display maximum 2PA cross sections within the narrow wavelength range.
- The 2PA cross section values enhanced in turn with the lengthen of the alkyl chain.
- The results of Lippert–Mataga equation are corresponding with optical properties.

GRAPHICAL ABSTRACT

A series of D-π-A type two-photon absorption organic salts based on pyridinium were and synthesized. Experimental results revealed the dyes possess the largest 2PA cross sections in the near infrared region (NIR) and display maximum two-photon absorption cross sections within the narrow wavelength range from 950 to 970 nm. Furthermore, the 2PA cross section values present enhanced trend in turn with the lengthen of the alkyl chain. In addition, we used the Lippert–Mataga equation to evaluate the dipole moment changes of the dyes with photoexcitation, the results are corresponding with linear and nonlinear optical properties of the dyes.

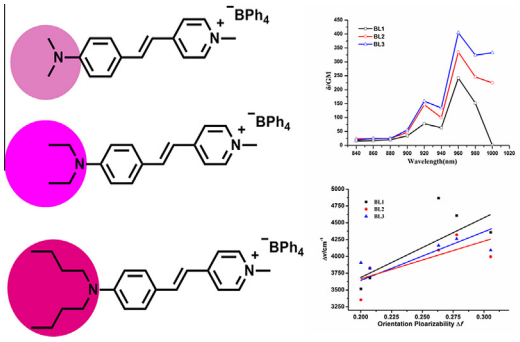

ARTICLE INFO

Article history:
Received 20 September 2013
Received in revised form 18 November 2013
Accepted 5 December 2013
Available online 18 December 2013

Keywords:
Stilbazolium
Donor-π-acceptor
Optical properties
Two-photon absorption
2PA cross section
Near-infrared

ABSTRACT

A series of stilbazolium salts based on donor-π-acceptor (D-π-A) structure have been synthesized and fully characterized. Photophysical properties including linear absorption, one-photon excited fluorescence (OPEF), two-photon absorption (2PA) properties were systematically investigated. The results suggest that increasing electron-releasing character of the terminal group leads to a more pronounced donor-to-acceptor intramolecular charge transfer (ICT). In addition, the dyes possess the largest 2PA cross sections in the near infrared region (NIR) and display maximum two-photon absorption cross sections within the narrow wavelength range from 950 to 970 nm and **BL3** exhibits a large nonlinear refractive index coefficient and possesses very large values of the real part of the cubic hyperpolarizability $\chi^{(3)}$ at 960 nm. Furthermore, the initial density functional theory (DFT) and time-dependent density functional theory (TD-DFT) calculations provide reasonable explanations for their absorption spectra, meanwhile we used the Lippert–Mataga equation to evaluate the dipole moment changes of the dyes with photoexcitation, the results are corresponding with linear and nonlinear optical properties of the dyes.

* Corresponding author. Tel.: +86 5582596249.
E-mail address: yxf301129@163.com (F. Hao).

1386-1425/$ - see front matter © 2013 Elsevier B.V. All rights reserved.
http://dx.doi.org/10.1016/j.saa.2013.12.048

Introduction

Optical materials with striking two-photon absorption effect have been the focus of intense current research. Such materials are of great scientific and technologic interest for applications in the areas of data processing, up-converted lasing, three-dimensional fluorescence microscopy, biological imaging [1–8]. All the applications depend critically on the availability of new materials with high two-photon absorption (2PA) cross sections. Therefore, significant effort has been devoted to the development of them.

The promise of diverse applications has stimulated many studies with organic 2PA materials over recent years. For those 2PA-based applications, the demand for rationally designed organic compounds that exhibit sufficiently large 2PA cross section is consequently escalating. The combination of several structural parameters, such as increasing the internal charge transfer and dimensionality of the molecule/extending π-conjugated system within a molecule, is closely related to molecular 2PA [9–12]. Stilbazolium salts are the best studied amongst such materials [13–16].

Up to now, there are many molecular design strategies were put forward to provide guidelines for the development of stilbazolium salts with large 2PA cross sections. In this context, we launched a program changing the phenylamine substituents which were introduced to molecules as the donor, and the molecular π-electron conjugated system was enlarged by forming —CH=CH— in 4-position of phenylamine. The cationic pyridinium unit as acceptor groups were bound on other side of vinyl bond. These dyes show negative solvatochromism in absorption spectra. Furthermore, they exhibits peak intense two-photon fluorescence-emission within narrow wavelength range.

Experiments

General

All chemicals used were of analytical grade and the solvents were purified by conventional methods before use. The ^{1}H NMR spectra were performed on Bruker 400 MHz spectrometer with TMS as the internal standard. Elemental analysis was performed on Perkin–Elmer 240 instrument. Mass spectra were determined with a Micromass GCT-MS (ESI source). IR spectra were recorded on NEXUS 870 (Nicolet) spectrophotometer in the 400–4000 cm^{-1} region using a powder sample on a KBr plate.

Optical measurements

The one-photon absorption (OPA) spectra were obtained on a UV-265 spectrophotometer. The one-photon excited fluorescence (OPEF) spectra measurements were performed using a Hitachi F-7000 fluorescence spectrophotometer. OPA and OPEF of **BL1–BL3** were measured in solvents of different polarities with the concentration of 2.0×10^{-6} mol L^{-1}. The quartz cuvettes used are of 1 cm path length. The fluorescence quantum yields (Φ) were determined by using Rh6G (in ethanol, $\Phi = 0.94$) as the reference according to the literature method [17]. Quantum yields were corrected as follows:

$$\Phi_s = \Phi_r \left(\frac{A_r \eta_s^2 D_s}{A_s \eta_r^2 D_r} \right)$$

where the *s* and *r* indices designate the sample and reference samples, respectively, A is the absorbance at λ_{exc}, η is the average refractive index of the appropriate solution, and D is the integrated area under the corrected emission spectrum [18].

The TD-DFT {B3LYP[LANL2DZ]} calculations were performed on the optimized structure. All calculations were performed with the G03 software, the TDDFT calculation of the lowest 25 singlet–singlet excitation energies were calculated with a basis set composed of 6-31 G(d) for C N H O atoms.

For time-resolved fluorescence measurements, the fluorescence signals were collimated and focused onto the entrance slit of a monochromator with the output plane equipped with a photomultiplier tube (HORIBA HuoroMax-4P). The decays were analyzed by 'least-squares'. The quality of the exponential fits was evaluated by the goodness of fit (χ^2).

Two-photon absorption (2PA) cross-sections (δ) of the samples were obtained by two-photon excited fluorescence (TPEF) method [19] at femtosecond laser pulse and Ti: sapphire system (680–1080 nm, 80 MHz, 140 fs) as the light source. The samples were dissolved in DMSO at a concentration of 1.0×10^{-3} mol L^{-1}. The intensities of TPEF spectra of the reference and the samples were determined at their excitation wavelength. Thus, 2PA cross-section (δ) of samples was determined by the following equation:

$$\delta = \delta_{ref} \frac{\Phi_{ref}}{\Phi} \frac{c_{ref}}{c} \frac{n_{ref}}{n} \frac{F}{F_{ref}}$$

where the *ref* subscripts stand for the reference molecule (here Rh6G in ethanol solution at concentration of 1.0×10^{-3} mol L^{-1} was used as reference). δ is the 2PA cross-sectional value, c is the concentration of the solution, n is the refractive index of the solution, F is the TPEF integral intensities of the solution emitted at the exciting wavelength, and Φ is the fluorescence quantum yield. The δ_{ref} value of reference was taken from the literature [20].

BL1, BL2, BL3 were synthesized by the following reactions (shown in Fig. 1).

Synthesis

Preparation of 1,4-dimethylpyridinium iodide

1,4-Dimethylpyridinium iodide was synthesized according to the literature method [21]. White powder product **4** was collected. Yield 90%. Mp: 155 °C. IR (KBr, cm^{-1}) selected bands: 3451 (m), 3023 (m), 1644 (s), 1517(m), 1517 (m), 1477 (m), 1289 (s), 1182 (s), 1043 (m), 809 (s), 697 (s), 485 (s). ^{1}H NMR (400 MHz, d_6-DMSO): 2.61 (3H, s), 4.29 (3H, s), 7.97 (2H, d, J = 6.4 Hz), 8.84 (2H, d, J = 6.4 Hz); M$^+$(MS/ESI), 108.48.

Preparation of substituted aminobenzaldehydes

4-(N, N-Dialkylamino)benzaldehyde was synthesized according to the literature method [22]. At room temperature, the compounds are pale yellow oil. For *4-(N, N-diethylamino)benzaldehyde,* IR (KBr, cm^{-1}) 2974 (m), 1665 (s), 1598 (s), 1566 (m), 1528 (s), 1470 (m), 1409 (s), 1357 (s), 1330 (m), 1179 (s), 1002 (w), 839 (m), 591 (w); ^{1}H NMR (400 MHz, d_6-acetone), d (ppm): 1.19 (6H, t, J = 7.0 Hz), 3.51(4H, m), 6.80 (2H, d, J = 8.8 Hz), 7.69 (2H, d, J = 9.2 Hz), 9.68 (1H, s). For *4-(N, N-dibutylamino)-benzaldehyde,* IR (KBr, cm^{-1}) selected bands: 2958 (s), 2931 (m), 2871 (m), 1669 (s), 1596 (s), 1525 (s), 1464 (w), 1405 (s), 1367 (s), 1313 (w), 1224 (m), 1168 (s), 814 (s), 607 (m), 510 (m); ^{1}H NMR (400 MHz, d_6-acetone), d (ppm): 0.94 (6H, t), 1.38 (4H, m), 3.40 (4H, m), 3.42 (4H, t), 6.76 (2H, d,), 7.65 (2H, d), 9.67 (1H, s).

Preparation of ***BL1***

BL1 was synthesized according to the literature method [23], red solid was collected. Yield: 96%. FT-IR (KBr, cm^{-1}) v: 2922 (w), 1643 (w), 1589 (s), 1521 (m), 1475 (w), 1437 (w), 1373 (m), 1330 (m), 1163 (s), 1037 (m), 708 (m). ^{1}H NMR (400 MHz, d_6-CD_3-$COCD_3$): 8.68 (d, 2H), 8.04 (d, 2H), 7.90 (d, 1H), 7.18–7.17 (q, 9H), 6.94–6.90 (t, 8H), 6.80–6.77 (t, 6H), 4.17 (s, 3H), 3.02 (s, 6H); M$^+$

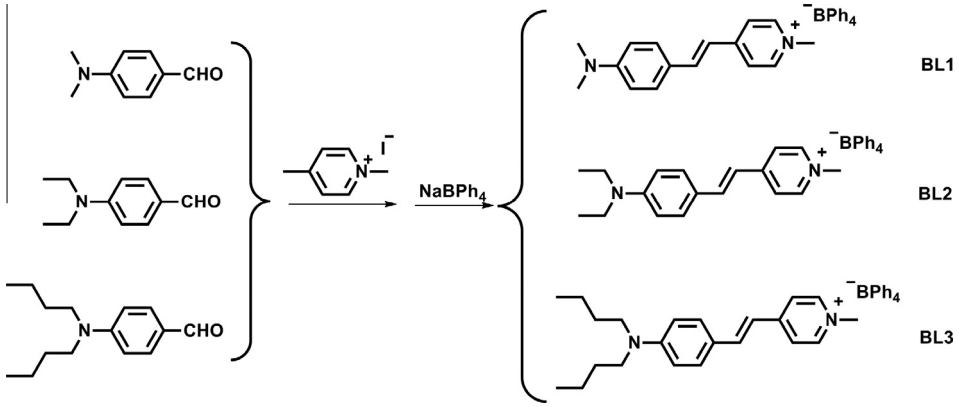

Fig. 1. The synthesis routes of target compounds.

(MS/ESI), 239.251. Anal. Calc. for $C_{40}H_{39}BN_2$: C, 86.01; H, 7.04; N, 5.02. Found: C, 86.04; H, 7.08; N, 5.07.

*Preparation of **BL2***

BL2 was synthesized according to the literature method [24], red solid was collected. Yield: 95%. FT-IR (KBr, cm^{-1}): 2968 (w), 1643 (w), 1584 (s), 1525 (s), 1468 (w), 1434 (w), 1408 (m), 1327 (m), 1172 (s), 1152 (s), 1037 (m), 706 (m). ^1H NMR (400 MHz, CD_3COCD_3-d_6): 8.62 (d, 2H), 8.04 (d, 2H), 7.89 (d, 1H), 7.59 (d, 2H), 7.35 (s, 8H), 7.14 (d, 1H), 6.94–6.91 (t, 8H), 6.79–6.75 (q, 6H), 4.35 (s, 3H), 3.53–3.48 (q, 4H), 1.22–1.18 (t, 6H); M^+ (MS/ESI), 267.283. Anal. Calc. for $C_{42}H_{43}BN_2$: C, 85.99; H, 7.39; N, 4.78. Found: C, 86.02; H, 7.38; N, 4.82.

*Preparation of **BL3***

Using a 100 mL one-necked flask fitted with a stirrer and a condenser, 2.33 g (0.01 mol) 4-(N, N-dibutylamino)-benzaldehyde, 2.35 g (0.01 mol) of compound 1,4-Dimethylpyridinium iodide, and 30 mL of absolute ethanol were mixed. Five drops of piperidine were added to the mixture. Then the solution was heated to reflux for 4 h. After cooling, 3.46 g (0.01 mol) of sodium tetraphenylborate was added into the solution. The solution again was heated to reflux for 10 min. A red solid formed after cooling. The solution was filtered, and the solid was washed twice with ethanol and water, respectively. Red solid product **BL3** was collected. Yield: 90%. FT-IR (KBr, cm^{-1}): 2955 (w), 2927 (m), 2866 (w), 1643 (w), 1587 (s), 1525 (s), 1471 (w), 1404 (w), 1368 (m), 1327 (m), 1213 (m), 1172 (s), 1037 (m), 709 (m). ^1H NMR (400 MHz, CD_3COCD_3-d_6): 9.9 (s, 1H), 7.68 (d, 2H), 6.77 (d, 2H), 3.45–3.41 (t, 4H), 1.65–1.57 (q, 4H), 1.41–1.36 (q, 4H), 0.97–0.94 (t, 6H). M^+ (MS/ESI), 323.391. Anal. Calc. for $C_{46}H_{51}BN_2$: C, 85.96; H, 8.00; N, 4.36. Found: C, 85.98; H, 8.02; N, 4.38.

Results and discussion

Structural features

In these structures, the cationic pyridinium can offer net positive charge for the molecular, and the large conjugate system which is composed of phenylamine, vinyl and cationic pyridinium ensures the large ionic radius. In addition, we can learn from the crystal data of **BL1** in literature [23] and **BL2** in our previous work [24], the C—C bond lengths of **BL2** (C5—C7: 1.485 Å, C8—C9: 1.477 Å) which link the benzene ring and pyridine ring are located between the normal C=C double bond (1.32 Å) and C—C single bond (1.53 Å), which show that there is a highly π-electron delocalized system in **BL2**, it is the necessary condition for it bearing strong 2PA response. For another, the linkage between the benzene ring and pyridine ring for **BL2** are shorter than **BL1** (C8—C9: 1.513 Å, C4—C7: 1.545 Å). It suggests that dye **BL2** possesses a higher delocalization within the molecule and more charge-transfer features of the ground state in the solid state compared with those of the dye **BL1**, which make the dye highly promising candidates for two-photon absorption materials.

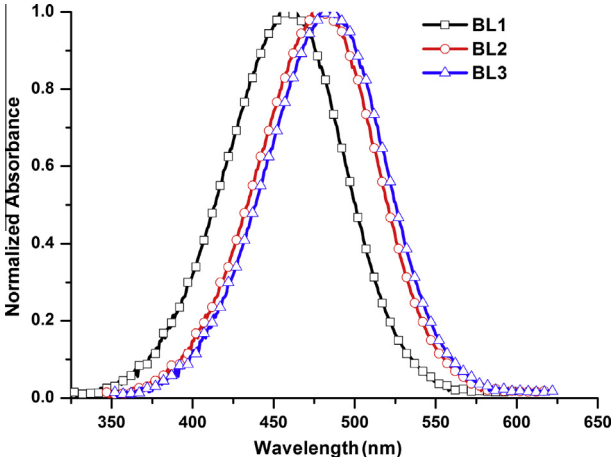

Fig. 2. Linear absorption spectra of all compounds in DMSO solution with 2×10^{-6} M.

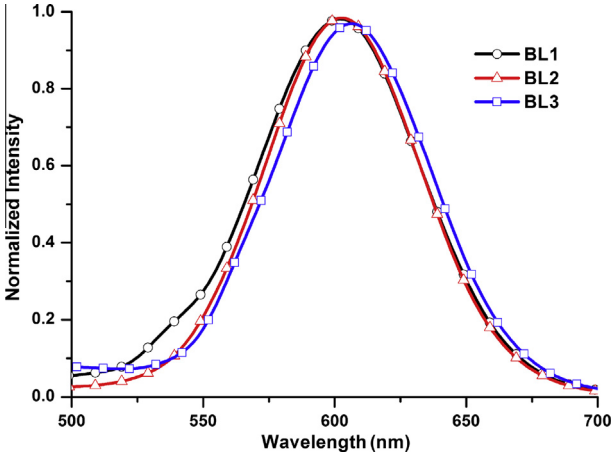

Fig. 3. One-photon excited fluorescence (right) spectra of all compounds in DMSO solution with 2×10^{-6} M.

Table 1
Photophysical properties of compounds **BL1–BL3** in several different solvents.

Compound	Solvents	λ_{max}[a] (ε_{max}[b])	λ_{max}[c]	Φ[d]	τ/ps[e]
	Ethyl acetate	479(2.74)	576	0.0451	105
	THF	476(3.92)	583	0.0203	289
	Ethanol	475(6.03)	590	0.0119	92
BL1	Methanol	473(5.22)	587	0.0048	41
	Acetonitrile	465(5.35)	599	0.0042	3
	DMF	465(5.47)	595	0.0043	68
	DMSO	464(4.80)	601	0.0072	97
	Ethyl acetate	490(2.43)	583	0.0094	152
	THF	494(4.65)	594	0.0137	166
	Ethanol	491(6.39)	590	0.0154	99
BL2	Methanol	483(7.12)	595	0.0034	56
	Acetonitrile	483(6.15)	606	0.0018	46
	DMF	483(4.76)	605	0.0068	89
	DMSO	479(5.92)	603	0.0126	137
	Ethyl acetate	479(2.34)	596	0.0108	196
	THF	480(2.75)	601	0.0184	231
	Ethanol	491(2.79)	596	0.0127	119
BL3	Methanol	486(2.69)	598	0.0043	85
	Acetonitrile	485(2.44)	606	0.0063	77
	DMF	484(2.87)	603	0.0116	116
	DMSO	483(2.57)	605	0.0059	179

[a] Peak position of the longest absorption band.
[b] Maximum molar absorbance in 10^4 mol^{-1} L cm^{-1}.
[c] Peak position of SPEF, exited at the absorption maximum.
[d] Quantum yields determined by using Rh6G as standard.

Linear optical properties

The UV–vis absorption and one-photon fluorescence spectra of the dyes in different solvents are shown in Figs. 2 and 3 and 1S–3S, and the relevant photophysical properties of these dyes are summarized in Table 1.

Linear absorption

As shown in Table 1, one can observe that absorption bands for all dyes feature one intense absorption band between 460 nm and 490 nm with the corresponding molar extinction coefficient (~50,000 M^{-1} cm^{-1}), which originates from the $\pi \rightarrow \pi^*$ or intramolecular charge transfer (ICT) transition. The bands exhibit slightly blue shifted in high polar solvents such as acetonitrile and DMF which is a feature of zwitterionic hemicyanine type dyes. This phenomenon is attributed to a relatively high polar mesomeric form, which is predominant in the ground state leading to a blue shift of the absorption band [25].

As shown in Fig. 2, for **BL1–BL3**, with the lengthen of the alkyl chain, the absorption bands exhibit slightly red shift in turn, this phenomenon might attributed to the substitution of the n-butyl (**BL3**) for methyl (**BL1**), ethyl (**BL2**) in phenylamine moiety which possesses higher electron-donating ability. The results suggest that increasing electron-releasing character of the terminal group leads to a more pronounced donor-to-acceptor ICT [26].

One-photon excited fluorescence (OPEF)

One can observe from Table 1, the fluorescence emission peaks for all dyes incline to red shift as the solvent polarity increase, indicating that the dipole moment of them in the excited states are larger than that in the ground states, and an increase in the polarity of the solvent will lower the energy level of the charge transfer excited states [27]. By comparison of the absorption spectral features of **BL1–BL3**, the fluorescence emission bands for them display a resemble regularity due to the electron-donating ability of the phenylamine group.

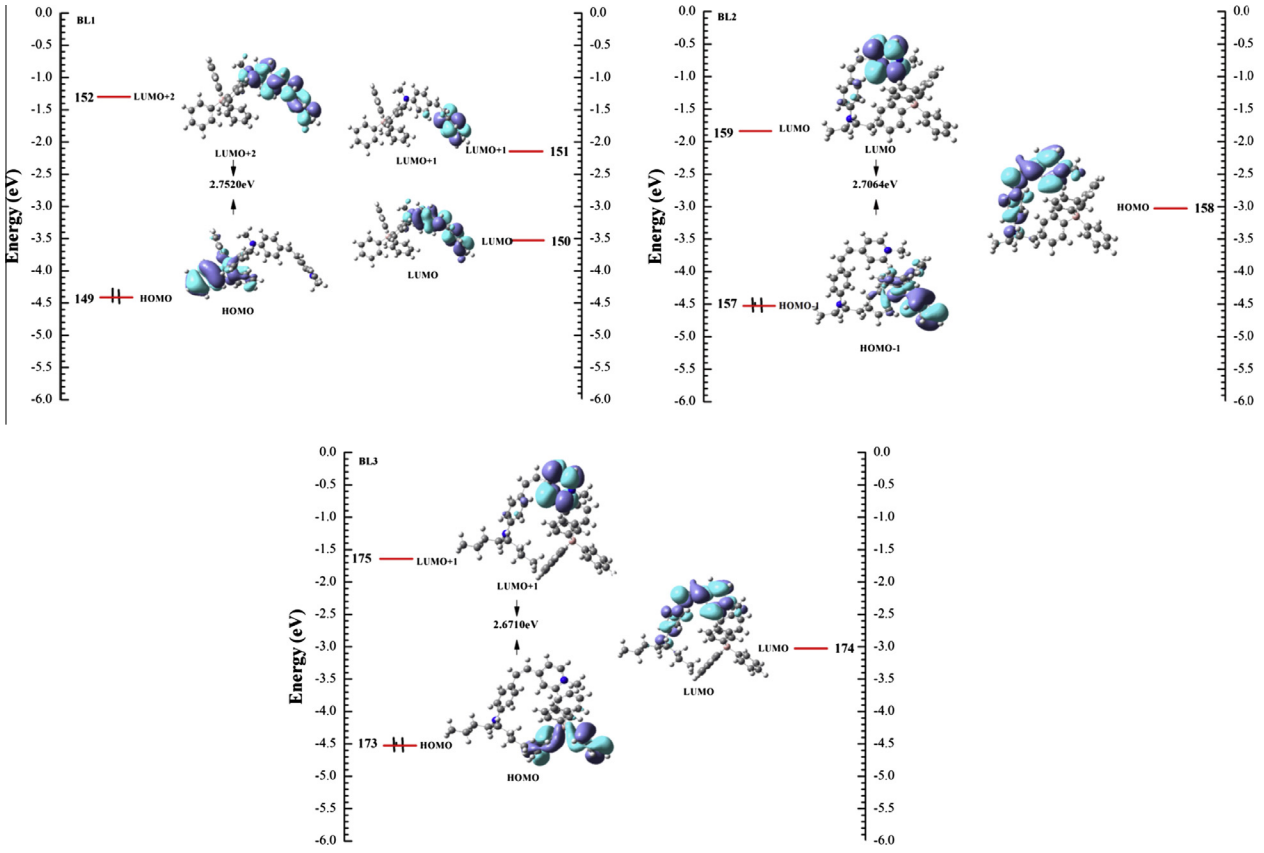

Fig. 4. Frontier molecular orbital diagrams for compounds **BL1–BL3**.

Table 2
Excitation energy (E), corresponding wavelength (λ), oscillator strength (f) and major contribution of **BL1–BL3**.

Compound	E (eV)	λ (nm)	f	Composition (C)	Character
BL1	2.7520	450.52	1.230	149(H) > 152(L + 2)(0.67982)	ICT
BL2	2.7064	465.56	1.2005	157(H-1) → 159(L)(0.64326)	ICT
BL3	2.6710	474.51	1.0078	173(H) → 175(L + 1)(0.54365)	ICT

Meanwhile it can be found that the photophysical properties of all dyes show low quantum yield (<10%). The behaviour is due to certain nonradiative decay mechanisms that may arise as a result of 'twisted intramolecular charge geometry' (TICT) [28]. From Table 1 we can observe that the fluorescence lifetime of these dyes is short, thereby supporting the assumption that because of the nonradiative decay arised as a result of TICT enhancing the quenching efficiency.

TD-DFT studies

TD-DFT computational studies were performed to elucidate the electronic structures of the ground state of **BL1–BL3**. The schematic representation of the molecular orbitals of them was exhibited in Fig. 4, and Table 2 shows the energy and composition of ICT. Fig. 4 shows the calculated frontier orbitals of **BL1–BL3**, the energy band were all tentatively assigned to ICT. Therefore the initial DFT and TD-DFT calculations provide reasonable explanations for their absorption spectra.

In addition, as we known, the most widely used to evaluate the dipole moment changes of the dyes with photoexcitation is the Lippert–Mataga equation [29],

$$\Delta v = \frac{2\Delta f}{4\pi\varepsilon_0 \hbar c a^3}(\mu_e - \mu_g)^2 + b \quad (1)$$

$$\Delta f = \frac{\varepsilon - 1}{2\varepsilon + 1} - \frac{n^2 - 1}{2n^2 + 1} \quad (2)$$

in which $\Delta v = v_{abs} - v_{em}$ stands for Stokes shift, v_{abs} and v_{em} are absorption and emission (cm^{-1}), $\hbar$ is the Planck's constant, c is the velocity of light in vacuum, a is the Onsager radius and b is a constant. Δf is the orientation polarizability, μ_e and μ_g are the dipole moments of the emissive and ground states, respectively and ε_0 is the permittivity of the vacuum. $(\mu_e - \mu_g)^2$ is proportional to the slope of the Lippert–Mataga plot.

Plots of the Stokes shifts as a function of the solvent polarity factor Δf are shown in Fig. 5. Only the data involving the aprotic solvents are shown because application of this analysis with solvents where specific solute–solvent interactions are present is not appropriate. As shown in Fig. 5, the slope of the best-fit line is related to the dipole moment change between the ground and excited states (μ_e–μ_g). The slopes of all three lines are different: 8566, 5711, and 6714 cm^{-1} for dye **BL1**, **BL2**, and **BL3**, respectively. So the values of μ_e–μ_g were calculated as 11.5 D for dye **BL1**, 16.5 D for dye **BL2**, and 18.6 D for dye **BL3**, respectively (Eq. (1)). The large values of dye **BL3** indicates that the molecule in the excited state has an extremely polar structure, especially for dye **BL3**, corresponding with their linear and nonlinear optical properties [30].

Two-photon excited fluorescence

As shown in Fig. 2, there is no linear absorption in the wavelength range 680–1200 nm for all the compounds in DMSO, which means that there are no energy levels corresponding to an electron transition in this spectral range. If frequency up-converted fluorescence appears upon excitation with a tunable laser in this range, it should be mainly attributed to TPEF. The spectra obtained by using the optical excitation wavelength 960 nm are shown in Fig. 6. In all the cases, the output intensity of two-photon excited fluorescence was linearly dependent on the input laser, thereby confirming the 2PA process (shown in Fig. 7).

As shown in Fig. 6, it can be seen clearly that the two-photon excited fluorescence intensity of **BL1–BL3** present enhanced trend in turn, which may due to the electron-donating ability of the terminal group. The growth of the alkyl chain increases the electron density of the bridge, favoring the ICT along the extended π bridge from terminal donor to acceptor group.

TPA cross-sections

As shown in Fig. 8, two-photon absorption cross sections (δ) of **BL1–BL3** were measured in the wide wavelength range from 840 to 1000 nm. The maximum values in DMSO are 242, 335 and 405 GM respectively (Table 3), which present enhanced trend in turn, this may due to the electron-donating ability of the terminal group as well. In addition, from these data, it can be observed that the

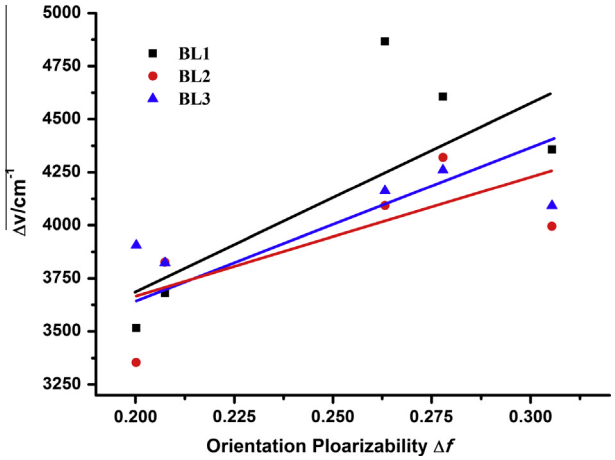

Fig. 5. Lippert–Mataga plots for **BL1–BL3**.

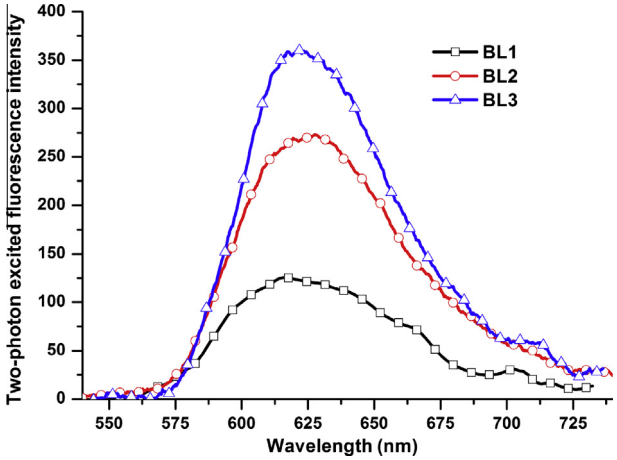

Fig. 6. The two-photon fluorescence spectra of **BL1–BL3** in DMSO ($c = 1.0 \times 10^{-3}$).

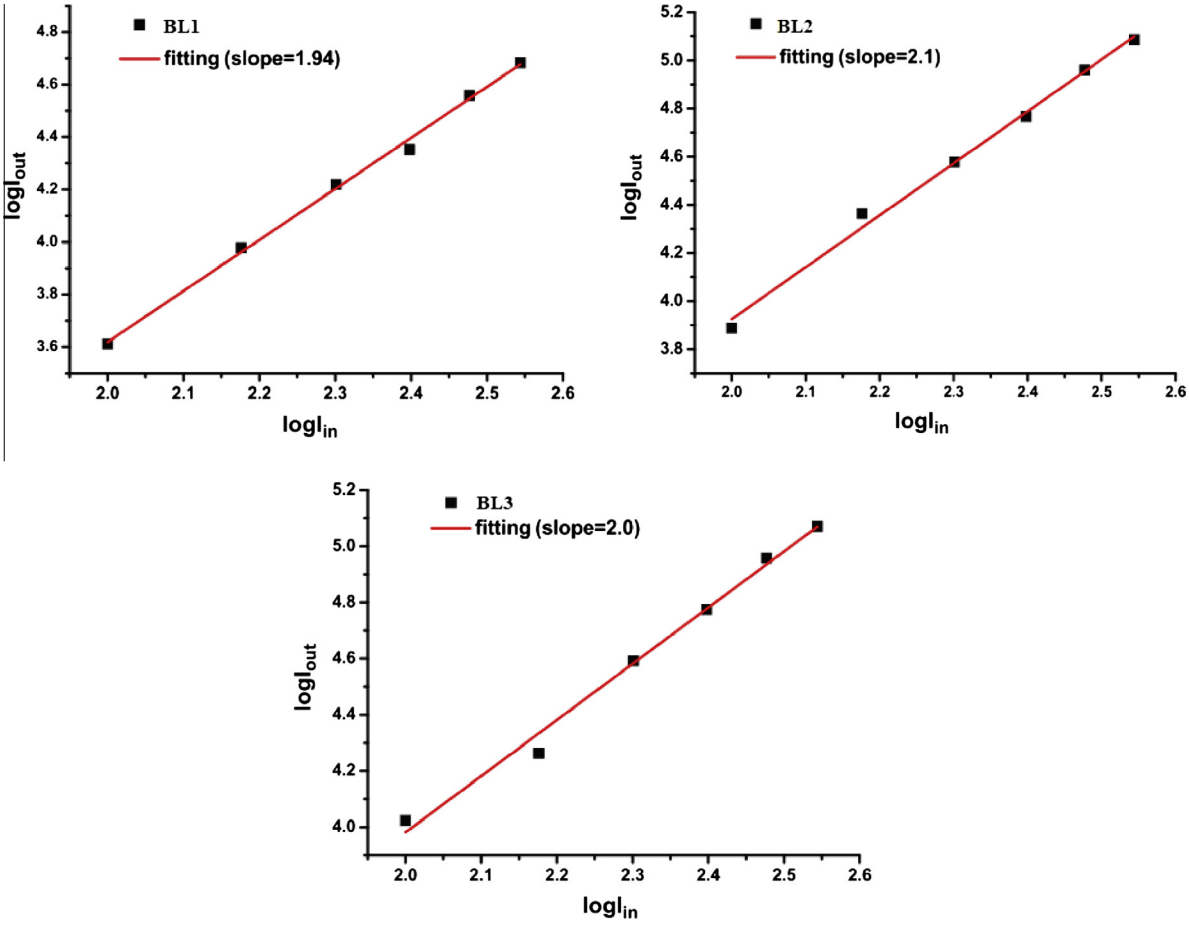

Fig. 7. Output fluorescence (I_{out}) vs. the square of input laser power (I_{in}) for **BL1**, **BL2**, and **BL3** excitation carried out at 960 nm, with $c = 1.0 \times 10^{-3}$ mol L^{-1} in DMSO, respectively.

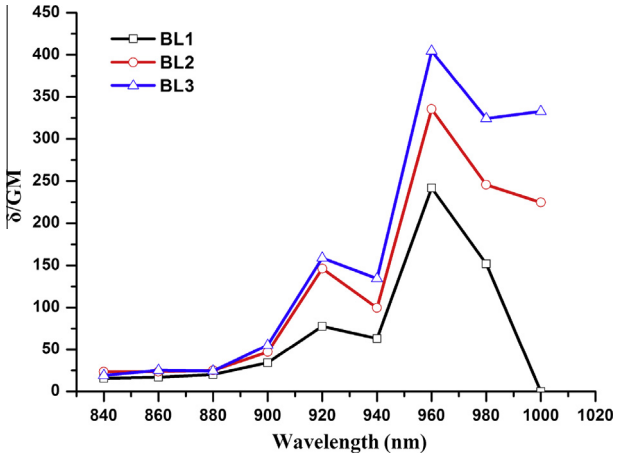

Fig. 8. Two-photon absorption cross sections of **BL1–BL3** in DMSO *vs* excitation wavelengths of identical energy of 0.300 W.

Table 3
The largest TPA cross section of **BL1–BL3** in DMSO vs. Excitation wavelength 960 nm.

Compound	BL1	BL2	BL3
δ/GM	242	335	405

dramatically larger two-photon absorption cross sections appear in the narrow pathlength about 950–970 nm, which is corresponding with our previous work [31], it may result from that there are excited-states (S_1–S_n) distributing in a much narrow energy band [32].

TPA coefficient β and $\chi^{(3)}$

Considering above, we singled out **BL3** which possessed the largest two-photon absorption cross sections (δ), the coefficient β and $\chi^{(3)}$ of **BL3** were measured by the Z-scan technique [33,34]. In the present experiments, a 1×10^{-3} M solution of **BL3** in DMSO contained in a 1.0 mm path-length quartz cell for Z-scan measurements was performed at 960 nm. The TPA coefficient β and $\chi^{(3)}$ calculation method can be obtained according to literature methods [35]. Fig. 9 shows the normalized transmittance plotted as a function of the sample position (z) measured by using open aperture and closed aperture Z-scan technique at 960 nm. Table 4 shows the third-order nonlinearity parameters of **BL3**. From these data, it can be seen that **BL3** exhibits a large nonlinear refractive index coefficient and possesses very large values of the real part of the cubic hyperpolarizability $\chi^{(3)}$ at 960 nm. This behaviour should establish the foundation for its device application [15(j)].

Conclusions

A series of D-π-A type two-photon absorption organic salts (**BL1**, **BL2**, and **BL3**) based on pyridinium were synthesized. Linear absorption, one/two-photon excited fluorescence behaviour and the excited-state lifetimes have been systematically investigated.

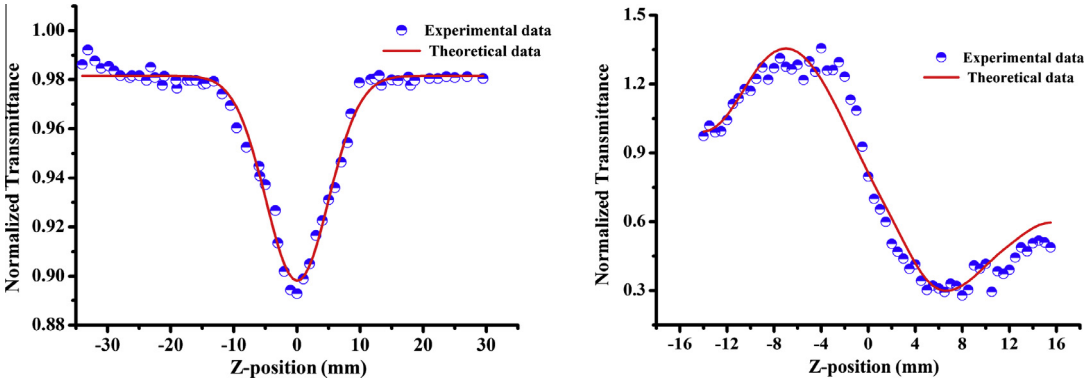

Fig. 9. Normalized open-aperture (left) and closed-aperture (right) Z-scan transmittance of **BL3** in DMSO (0.001 M) at 960 nm.

Table 4
Open- and closed-aperture Z-scan measurement data for the third-order nonlinearity parameters of **BL3**.

n_2 Extrapolated to solute (cm^2/W)	Re ($\chi^{(3)}$) extrapolated to solute (esu)	2PA coefficient α_2 (cm/GW) extrapolated to solute	Two-photon cross section σ (GM)	Im ($\chi^{(3)}$) extrapolated to solute (esu)
2.60×10^{-10}	1.44×10^{-12}	0.024	829.77	1.02×10^{-15}

The relationships between the structures and photophysical properties of them can be understood based on both the experimentally and theoretically. In the experimental part: it was found that the dyes showed solvent-polarity-dependent fluorescence in the visible region. In addition, the dyes possess the largest 2PA cross sections in the near infrared region (NIR) and display maximum two-photon absorption cross sections within the narrow wavelength range from 950 to 970 nm. Furthermore, the 2PA cross section values present enhanced trend in turn with the lengthen of the alkyl chain and **BL3** exhibits a large nonlinear refractive index coefficient and possesses very large values of the real part of the cubic hyperpolarizability $\chi^{(3)}$ at 960 nm. In the theoretical part: the initial DFT and TD-DFT calculations provide reasonable explanations for their absorption spectra, meanwhile the calculation results of the Lippert–Mataga equation are corresponding with linear and nonlinear optical properties of the dyes. The results reported in this paper provide a useful design and synthesis strategy for the two-photon absorbing materials.

Acknowledgements

This work was supported by the National Natural Science Foundation of China (20875001), Education Committee of Anhui Province (KJ2013B205, KJ2013B204).

Appendix A. Supplementary material

Supplementary data associated with this article can be found, in the online version, at http://dx.doi.org/10.1016/j.saa.2013.12.048.

References

[1] G.S. He, L.S. Tan, Q.D. Zheng, P.N. Prasad, Multiphoton absorbing materials: molecular designs, characterizations, and applications, Chem. Rev. 108 (2008) 1245–1330.
[2] M. Pawlicki, H.A. Collins, R.G. Denning, H.L. Anderson, Two-photon absorption and the design of two-photon dyes, Angew. Chem. Int. Ed. 48 (2009) 3244–3266.
[3] M.J. Therien, How to improve your image, Nature 458 (2009) 716–717.
[4] J.E. Reeve, H.A. Collins, K.D. Mey, M.M. Kohl, K.J. Thorley, O. Paulsen, K. Clays, H.L. Anderson, Amphiphilic porphyrins for second harmonic generation imaging, J. Am. Chem. Soc. 131 (2009) 2758–2759.
[5] J.M. Hales, Design of polymethine dyes with large third-order optical nonlinearities and loss figures of merit, Science 327 (2010) 1485–1488.
[6] S.A. Haque, J. Nelson, Toward organic all-optical switching, Science 327 (2010) 1466–1467.
[7] S. Sumalekshmy, C.J. Fahrni, Metal-ion-responsive fluorescent probes for two-photon excitation microscopy, Chem. Mater. 23 (2011) 483–500.
[8] Sheng Yao, Kevin D. Belfield, Two-photon fluorescent probes for bioimaging, Eur. J. Org. Chem. 17 (2012) 3199–3217.
[9] (a) A. Bhaskar, G. Ramakrishna, Z. Lu, R. Twieg, J.M. Hales, D.J. Hagan, et al., Investigation of two-photon absorption properties in branched alkene and alkyne chromophores, J. Am. Chem. Soc. 128 (2006) 11840–11849;
(b) A. Bhaskar, R. Guda, M.M. Haley, I.I.I. Theodore Goodson, Building symmetric two-dimensional two-photon materials, J. Am. Chem. Soc. 128 (2006) 13972–13973;
(c) M. Williams-Harry, A. Bhaskar, G. Ramakrishna, I.I.I. Theodore Goodson, M. Imamura, A. Mawatari, et al., Giant thienylene-acetylene-ethylene macrocycles with large two-photon absorption cross section and semishape-persistence, J. Am. Chem. Soc. 130 (2008) 3252–3253.
[10] (a) M. Rumi, J.E. Ehrlich, A.A. Heikal, J.W. Perry, S. Barlow, Z. Hu, et al., Structure-property relationships for two-photon absorbing chromophores: bis-donor diphenylpolyene and bis(styryl)benzene derivatives, J. Am. Chem. Soc. 122 (2000) 9500–9510;
(b) S.J. Chung, M. Rumi, V. Alain, S. Barlow, J.W. Perry, S.R. Marder, Strong, low-energy two-photon absorption in extended amine-terminated cyano-substituted phenylenevinylene oligomers, J. Am. Chem. Soc. 127 (2005) 10844–10845;
(c) S.J. Chung, S. Zheng, T. Odani, L. Beverina, J. Fu, L.A. Padilha, et al., Extended squaraine dyes with large two-photon absorption cross-sections, J. Am. Chem. Soc. 128 (2006) 14444–14445.
[11] (a) K.D. Belfield, A.R. Morales, J.M. Hales, D.J. Hagan, E.W.V. Stryland, V.M. Chapela, et al., Linear and two-photon photophysical properties of a series of symmetrical diphenylaminofluorenes, Chem. Mater. 16 (2004) 2267–2273;
(b) K.D. Belfield, D.J. Hagan, E.W.V. Stryland, K.J. Schafer, R.A. Negres, New two-photon absorbing fluorene derivatives: synthesis and nonlinear optical characterization, Org. Lett. 1 (1999) 1575–1578.
[12] (a) L. Porres, O. Mongin, C. Katan, M. Charlot, T. Pons, J. Mertz, et al., Enhanced two-photon absorption with novel octupolar propeller-shaped fluorophores derived from triphenylamine, Org. Lett. 6 (2004) 47–50;
(b) M. Drobizhev, F. Meng, A. Rebane, Y. Stepanenko, E. Nickel, C.W. Spangler, Strong two-photon absorption in new asymmetrically substituted porphyrins: interference between charge-transfer and intermediate-resonance pathways, J. Phys. Chem. B 110 (2006) 9802–9814.
[13] S.R. Marder, J.W. Perry, W.P. Schaefer, Synthesis of organic salts with large second-order optical nonlinearities, Science 245 (1989) 626–628.
[14] (a) B.J. Coe, J.A. Harris, K. Clays, A. Persoons, K. Wostyn, B.S. Brunschwig, A comparison of the pentaammine(pyridyl)ruthenium(II) and 4-(dimethylamino)phenyl groups as electron donors for quadratic non-linear optics, Chem. Commun. (2001) 1548–1549;
(b) B.J. Coe, J.A. Harris, I. Asselberghs, K. Clays, G. Olbrechts, A. Persoons, J.T.

Hupp, R.C. Johnson, S.J. Coles, M.B. Hursthouse, K. Nakatani, Quadratic nonlinear optical properties of N-aryl stilbazolium dyes, Adv. Funct. Mater. 12 (2002) 110–116;
(c) B.J. Coe, J.A. Harris, I. Asselberghs, K. Wostyn, K. Clays, A. Persoons, B.S. Brunschwig, S.J. Coles, T. Gelbrich, M.E. Light, M.B. Hursthouse, K. Nakatani, Quadratic optical nonlinearities of N-methyl and N-aryl pyridinium salts, Adv. Funct. Mater. 13 (2003) 347–357;
(d) K. Clays, B.J. Coe, Design strategies versus limiting theory for engineering large second-order nonlinear optical polarizabilities in charged organic molecules, Chem. Mater. 15 (2003) 642–648;
(e) E. Stathatos, P. Lianos, Synthesis of a hemicyanine dye bearing two carboxylic groups and its use as a photosensitizer in dye-sensitized photoelectrochemical cells, Chem. Mater. 13 (2001) 3888–3892.

[15] (a) C.F. Zhao, R. Gvishi, U. Narang, G. Ruland, PrasadPN, Structures, spectra, and lasing properties of new (aminostyryl)pyridinium laser dyes, J. Phys. Chem. 100 (1996) 4526–4532;
(b) U. Narang, C.F. Zhao, J.D. Bhawalkar, F.V. Bright, P.N. Prasad, Characterization of a new solvent-sensitive two-photon-induced fluorescent (aminostyryl)pyridinium salt dye, J. Phys. Chem. 100 (1996) 4521–4525;
(c) B.A. Reinhardt, L.L. Brott, S.J. Clarson, A.G. Dillard, J.C. Bhatt, P.N. Prasad, et al., Highly active two-photon dyes: design, synthesis, and characterization toward application, Chem. Mater. 10 (1998) 1863–1874;
(d) M. Lal, L. Levy, K.S. Kim, G.S. He, X. Wang, Y.H. Min, S. Pakatchi, P.N. Prasad, Silica nanobubbles containing an organic dye in a multilayered organic/inorganic heterostructure with enhanced luminescence, Chem. Mater. 12 (2000) 2632–2639;
(e) R. Kannan, G.S. He, L. Yuan, F. Xu, P.N. Prasad, A.G. Dombroskie, et al., Diphenylaminofluorene-based two-photon-absorbing chromophores with various π-electron acceptors, Chem. Mater. 13 (2001) 1896–1904;
(f) Q.D. Zheng, G.S. He, T.C. Lin, P.N. Prasad, Synthesis and properties of substituted (p-aminostyryl)-1-(3-sulfooxypropyl)pyridinium inner salts as a new class of two-photon pumped lasing dyes, J. Mater. Chem. 13 (2003) 2499–2504;
(g) R. Kannan, G.S. He, T.C. Lin, P.N. Prasad, R.A. Vaia, L.S. Tan, Toward highly active two-photon absorbing liquids. synthesis and characterization of 1,3,5-triazine-based octupolar molecules, Chem. Mater. 16 (2004) 185–194;
(h) T.C. Lin, G.S. He, P.N. Prasad, L.S. Tan, Degenerate nonlinear absorption and optical power limiting properties of asymmetrically substituted stilbenoid chromophores, J. Mater. Chem. 14 (2004) 982–991;
(i) Q. Zheng, G.S. He, P.N. Prasad, π-Conjugated dendritic nanosized chromophore with enhanced two-photon absorption, Chem. Mater. 17 (2005) 6004–6011;
(j) G.S. He, J. Zhu, A. Baev, M. Samo, D.L. Frattarelli, N. Watanabe, A. Facchetti, H. Ågren, T.J. Marks, P.N. Prasad, Twisted π-system chromophores for all-optical switching, J. Am. Chem. Soc. 133 (2011) 6675–6680.

[16] (a) X.J. Zhang, Y.P. Tian, F. Jin, J.Y. Wu, Y. Xie, X.T. Tao, M.H. Jiang, Self-assembly of an organic chromophore with Cd-S nanoclusters: supramolecular structures and enhanced, Cryst. Growth Des. 5 (2005) 565–570;
(b) F.Y. Hao, X.J. Zhang, Y.P. Tian, H.P. Zhou, L. Li, J.Y. Wu, et al., Design, crystal structures and enhanced frequency-upconverted lasing efficiencies of a new series of dyes from hybrid of inorganic polymers and organic chromophores, J. Mater. Chem. 19 (2009) 9163–9169;
(c) Y.P. Tian, L. Li, Y.H. Zhou, P. Wang, Y.H. Zhou, J.Y. Wu, et al., Design and synthesis of two new two-photon absorbing pyridine salts as ligands and their rare earth complexes, Cryst. Growth Des. 9 (2009) 1499–1504;
(d) J.Y. Wu, G.J. Hu, P. Wang, F.Y. Hao, H.P. Zhou, Y.P. Tian, et al., Organic/polyoxometalate hybridization dyes: crystal structure and enhanced two-photon absorption, Dyes Pig. 88 (2010) 174–179.

[17] J.N. Demas, G.A. Crosby, The measurement of photoluminescence quantum yields, J. Phys. Chem. 75 (1971) 991–1024.

[18] T.G. Gray, C.M. Rudzinski, E.E. Meyer, R.H. Holm, D.G. Nocera, Spectroscopic and photophysical properties of hexanuclear rhenium(III) chalcogenide clusters, J. Am. Chem. Soc. 125 (2003) 4755–4770.

[19] S.K. Lee, W.J. Yang, J.J. Choi, C.H. Kim, S.J. Jeon, B.R. Cho, 2,6-Bis[4-(p-dihexylaminostyryl)-styryl]anthracene derivatives with large two-photon cross sections, Org. Lett. 7 (2005) 323–326.

[20] C. Xu, W.W. Webb, Measurement of two-photon excitation cross sections of molecular fluorophores with data from 690 to 1050 nm, J. Opt. Soc. Am. B 13 (1996) 481–491.

[21] C.F. Zhao, G.S. He, J.D. Bhawalkar, C.K. Park, P.N. Prasad, Newly synthesized dyes and their polymer/glass composites for one- and two-photon pumped solid-state cavity lasing, Chem. Mater. 7 (1995) 1979–1983.

[22] (a) C.F. Zhao, G.S. He, J.D. Bhawalkar, C.K. Park, P.N. Prasad, Newly synthesized dyes and their polymer/glass composites for one- and two-photon pumped solid-state cavity lasing, Chem. Mater. 7 (1995) 1979–1983;
(b) C.F. Zhao, C.K. Park, P.N. Prasad, Y. Zhang, S. Ghosal, R. Burzynski, Photorefractive polymer with side-chain second-order nonlinear optical and charge-transporting groups, Chem. Mater. 7 (1995) 1237–1242.

[23] S.J. Li, D.C. Zhang, Z.L. Huang, Y.Q. Zhang, K.B. Yu, 4-[2-(4-Methoxyphenyl) ethenyl]-N-methylpyridinium tetraphenylborate, Chin. J. Struct. Chem. 19 (2000) 263–266.

[24] D.D. Li, R. Li, S.L. Li, 4-(E)-2-[4-(Diethylamino) phenyl] ethenyl-1-methylpyridin-1-ium tetraphenylborate, Acta Cryst. E68 (2012) o2694.

[25] M. Lal, L. Levy, K.S. Kim, Silica nanobubbles containing an organic dye in a multilayered organic/inorganic heterostructure with enhanced luminescence, Chem. Mater. 12 (2000) 2632–2639.

[26] H.M. Kim, B.R. Cho, Two-photon materials with large two-photon cross sections. Structure-property relationship, Chem. Commun. (2009) 153–164.

[27] X.M. Wang, D. Wang, G.Y. Zhou, W.T. Yu, Y.F. Zhou, Q. Fang, et al., Symmetric and asymmetric charge transfer process of two-photon absorbing chromophores: bis-donor substituted stilbenes, and substituted styrylquinolinium and styrylpyridinium derivatives, J. Mater. Chem. 11 (2001) 1600–1605.

[28] C. Rullière, Z.R. Grabowski, J. Dobkowski, Picosecond absorption spectra of carbonyl derivatives of dimethylaniline: the nature of the tict excited states, Chem. Phys. Lett. 137 (1987) 408–413.

[29] (a) S.A. Patel, M. Cozzuol, J.M. Hales, C.I. Richards, M. Sartin, J.C. Hsiang, T. Vosch, J.W. Perry, R.M. Dickson, Electron transfer-induced blinking in Ag nanodot fluorescence, J. Phys. Chem. C 113 (2009) 20264–20270;
(b) S.M. Ji, J. Yang, Q. Yang, S.S. Liu, M.D. Chen, J.Z. Zhao, Tuning the intramolecular charge transfer of alkynylpyrenes: effect on photophysical properties and its application in design of off–on fluorescent thiol probes, J. Org. Chem. 74 (2009) 4855–4865.

[30] M. Irie, K. Sayo, Solvent effects on the photochromic reactions of diarylethene derivatives, J. Phys. Chem. 96 (1992) 7671–7674.

[31] D.D. Li, D.H. Yu, Q. Zhang, S.L. Li, H.P. Zhou, J.Y. Wu, Y.P. Tian, Synthesis, crystal structure and third-order nonlinear optical properties in the near-IR range of a novel stilbazolium dye substituted with flexible polyether chains, Dyes Pigments 97 (2013) 278–285.

[32] M. Johnsen, P.R. Ogilby, Effect of solvent on two-photon absorption by vinyl benzene derivatives, J. Phys. Chem. A 112 (2008) 7831–7839.

[33] M. Sheik-Bahae, A.A. Said, T.H. Wei, D.J. Hagan, E.W. Van Stryland, Sensitive measurement of optical nonlinearities using a single beam, IEEE J. Quantum Electron. 26 (1990) 760–769.

[34] W. Zhao, P. Paltty-Muhoray, Z-scan measurement of $\chi^{(3)}$ using top-hat beams, Appl. Phys. Lett. 65 (1994) 673–675.

[35] S.L. Li, J.Y. Wu, Y.P. Tian, Y.W. Tang, M.H. Jiang, H.K. Fun, Preparation, characterization, two-photon absorption and optical limiting properties of a novel metal complex containing carbazole, Opt. Mater. 28 (2006) 897–903.